

# Supplemental Information to

## Motif mimetic of epsin perturbs tumor growth and metastasis

**Authors:** Yunzhou Dong<sup>1,\*</sup>, Hao Wu<sup>1</sup>, H. N. Ashiqur Rahman<sup>1</sup>, Yanjun Liu<sup>2</sup>, Satish Pasula<sup>1</sup>, Kandice L. Tessneer<sup>1</sup>, Xiaofeng Cai<sup>1</sup>, Xiaolei Liu<sup>1,3</sup>, Baojun Chang<sup>1</sup>, John McManus<sup>1</sup>, Scott Hahn<sup>1</sup>, Jiali Dong<sup>1</sup>, Megan L. Brophy<sup>1,3</sup>, Lili Yu<sup>1</sup>, Kai Song<sup>1</sup>, Robert Silasi-Mansat<sup>1</sup>, Debra Saunders<sup>4</sup>, Charity Njoku<sup>4</sup>, Padmaja Mehta-D'Souza<sup>1</sup>, Rheal Towner<sup>4</sup>, Florea Lupu<sup>1</sup>, Rodger P. McEver<sup>1,3</sup>, Lijun Xia<sup>1,3</sup>, Derek Boerboom<sup>5</sup>, R. Sathish Srinivasan<sup>1</sup> and Hong Chen<sup>1,3\*</sup>

### Affiliations:

<sup>1</sup> Cardiovascular Biology Program, Oklahoma Medical Research Foundation (OMRF), 825 NE 13<sup>th</sup> Street, Oklahoma City, OK 73104, USA

<sup>2</sup> Charles R. Drew University of Medicine & Sciences, University of California, 1731 E. 120th St, Los Angeles, CA 90059

<sup>3</sup> Department of Biochemistry and Molecular Biology, University of Oklahoma Health Sciences Center, Oklahoma City, OK 73104, USA.

<sup>4</sup> Advanced Magnetic Resonance Center, OMRF, Oklahoma City, OK 73104, USA.

<sup>5</sup> Département de Biomédecine Vétérinaire, Université de Montréal, 3200 Sicotte, St-Hyacinthe (Québec), J2S 7C6, Canada

\*Correspondence should be addressed to

Hong Chen, [hong-chen@omrf.org](mailto:hong-chen@omrf.org); Tel: 405-271-2750 and

Yunzhou Dong, [yunzhou-dong@omrf.org](mailto:yunzhou-dong@omrf.org); Tel: 405-271-2755

**Online-Only Extended Experimental Procedures, Supplemental Figure Legends 1-8 and Supplemental Table 1.**

## **Online-Only Extended Experimental Procedures**

### **Antibodies, reagents and chemicals**

Polyclonal rabbit antibodies for epsins 1 and 2 were obtained as previously described (17, 66). Epsin 1 antibody (goat, cat# sc-8673) was purchased from Santa Cruz Biotechnology Inc. (Santa Cruz, CA). Anti-VEGFR2 (cat# 2479), Anti-phospho-VEGFR2 (cat# 2478), anti-PLC $\gamma$  (cat# 2822), anti-phospho-PLC $\gamma$  (cat# 2821), anti-ERK (cat# 4695), anti-phospho-ERK (cat# 9106), anti-AKT (cat# 9272), anti-phospho-AKT (cat# 9271), anti-PDGFR- $\beta$  (cat# 3175) and anti-Snail (cat# 3879) antibodies were purchased from Cell Signaling Technology (Danvers, MA). Anti-phospho-VEGFR2 (pY1054/1059) antibody (cat# GTX25473) was purchased from Gene Tex (Irvine, CA). Anti-FGFR1 (cat# ab823) antibody was purchased from Abcam (San Francisco, CA). Anti-EGFR antibody (cat# 600-401-905) was purchased from Rockland Immunochemicals (Pottstown, PA). Anti-vimentin antibody (Clone Vim 3B4) was purchased from Dako (Carpinteria, CA). VEGF-A, FGF and PDGF were purchased from R&D systems (Minneapolis, MN). VEGFR2 kinase inhibitor was purchased from Calbiochem (San Diego, CA). BrdU and 4-hydroxytamoxifen were purchased from Sigma (St. Louis, MO). Anti-CD31 (cat# 550274) antibody and matrigel were purchased from BD Biosciences (San Jose, CA). Anti-Ve-cadherin antibody (cat# Vli37) was bought from Der-Antibody (Portland, ME). Integrin  $\alpha$ v and  $\beta$ 3 plasmids were purchased from Addgene (Cambridge, MA). All other chemicals were purchased from Sigma or elsewhere. Anti-VEGF (Clone B20-4.1.1) antibody was a kind gift from Genentech (South San Francisco, California).

### **Peptide synthesis**

Peptides were synthesized by Fmoc solid phase. Briefly, 2-Chlorotrityl Chloride resin (1.05 mMole/g substitution) was allowed to swell in DCM for 30 min, then the amino acid coupling

was performed. During this process, the generation and consumption of free primary amine was monitored through ninhydrin test. The deprotection and coupling sequence was repeated until the desired length of peptide was maintained, then the conjugate was cleaved using a cleavage mixture (95% TFA in the presence of TIS and EDT) for 2 hours at room temperature. The cleaved product was precipitated using cold ether. The crude product was then dissolved in a certain proportion of H<sub>2</sub>O and ACN. The crude sequence was qualitatively analyzed by 220nm on HPLC system using a Waters C-18 reverse phase column. The crude sequence was in a H<sub>2</sub>O:ACN gradient with ACN starting at a reasonable gradient. The purified fractions were collected and masses were confirmed using an API150-ESI mass spectrometry system. After confirmation, the products were further HPLC purified and lyophilized. Peptides were dissolved in purified H<sub>2</sub>O. Peptide endotoxin (EU/mg) was monitored using LAL kit (Pierce) per manufacturer's instructions.

### **Animal models**

All animal protocols have been approved by the IACUC in Oklahoma Medical Research Foundation. C56BL/6 mice and TRAMP prostate cancer models were obtained from Jackson Laboratory (Bar Harbor, Maine). SCID/NOD immune-deficient mice were purchased from Charles River Labs (Wilmington, MA). WT-Flk-1<sup>+/-</sup>, EC-iDKO, EC-iDKO-Flk-1<sup>+/-</sup> and EC-iDKO-Notch mice were generated by crossing conditional double knockout mice (EC-iDKO) with Flk-1<sup>fl/fl</sup> or NICD<sup>LSL</sup> mice as described (Supplemental Figure 5a) (17, 18).

Animal tumor models were established as follows:

(1) *Subcutaneous Tumor Models (LLC, melanoma B16 and glioma U87/SCID)*: Lewis lung carcinoma (LLC), B16F10 (B16) melanoma and glioma U87/SCID cells were purchased from ATCC and tumor models were established as previously described (17). Synthetic peptides were

administered at 10 mg/kg intravenously every-second-day beginning after small tumors were established (20-50 mm<sup>3</sup>; approximately 12 days post implantation). Tumor volumes were monitored every-other-day until euthanized following IACUC tumor scoring system. (2) *TRAMP Prostate Tumor Model* (Transgenic Adenocarcinoma of Mouse Prostate, bought from Jackson Laboratory): Mice aged 20 weeks received control (CTR) or UPI peptides by intraperitoneal injection every-second-day (20 mg/kg) until the mice died or were euthanized following IACUC tumor scoring system. Mortality rates were recorded. Prostate tumors were analyzed by weighing genitourinary tract (GU), H&E staining, immunofluorescence staining and Western blotting as previously described (17, 54). Lung and liver were similarly analyzed for metastasis. (3) *B16 Melanoma Metastasis Model*: 1 x 10<sup>6</sup> B16 melanoma cancer cells were subcutaneously implanted into C56BL/6 mice. Established tumors (400-500 mm<sup>3</sup>) were surgically removed then CTR or UPI peptides were intravenously injected every-second-day (10 mg/kg) for five weeks. Mice were sacrificed after 5 weeks and tissues (including lung, liver and lymph nodes, etc) were harvested and analyzed for metastasis by gross morphology, H&E staining, immunofluorescence staining and Western blotting. (4) *Orthotopic Glioma Tumor Models (U87/SCID and GL261/C56BL/6)*: Orthotopic glioma models were established by implanting U87 or GL261 glioma cells in the forebrain of SCID or C57BL/6 mice, respectively, as previously described (55). Tumors were monitored by MRI as previously described (17). Once tumors reached 10-20 mm<sup>3</sup> in size, CTR or UPI peptides were administered intravenously every-second-day (10 mg/kg). Tumor volume was analyzed by MRI every-other-day until the mice died or were euthanized following IACUC tumor scoring system. Mortality rates were recorded. Anti-VEGF antibody (B20-4.1.1) served as positive control (5 mg/kg).

#### **Co-administration of UPI or anti-VEGF antibody with cytotoxic chemotherapeutics**

(1) Subcutaneous LLC tumor-bearing mouse models were established as stated. UPI peptide (8 mg/kg) or anti-VEGF antibody (2.5 mg/kg) was co-administrated with cytotoxic chemotherapeutics, doxorubicin (Dox) (10 mg/kg) or Taxol (Tax) (5 mg/kg). UPI, anti-VEGF antibody or Dox was intravenously injected while Tax was intraperitoneal injected. All agents were administrated every-other-day.

(2) GL261 glioma tumor models were established in WT C57BL/6 as described above (55) by OMRF researcher Dr. Rheal Towner group. UPI (5 mg/kg) or anti-VEGF antibody (2.5 mg/kg) was delivered by intravenous injection every-other-day. OKN-007 added to the drinking water at 0.1% w/v (or 75 mg/kg/day) as previously established (38).

#### **Isolation of tumor endothelial cells (TEC) from LLC tumors**

Subcutaneous LLC tumors were established as stated above and harvested when the tumor diameter reached ~1cm. Tumors were digested in enzymatic buffer (10 mg/ml Collagenase, 5 mg/ml Dispase and 1 mg/ml DNase in DMEM medium) and minced by passing through an 18G needle four times. A second round of digestion in the same enzymatic buffer in a 37°C water bath for 1 hour was done, followed by mincing with a 21G and 25G needle. Cells were filtered using a 100 µm strainer then  $4 \times 10^7$  cells were used for TEC isolation using a magnetic cell sorting system and the MACS protocol described by Miltenyl Biotec. Leukocyte, platelets, and macrophages, which may also express CD31, were first depleted by CD45 microbeads. In the CD45-negative population, anti-mouse CD31 microbeads were added and incubated for 15 min rotation at 4°C. CD31-positive cells were sorted and plated onto 0.5% gelatin-coated culture plates and grown in endothelial culture medium supplemented with 15% FBS. Diphtheria toxin (DT) (500 ng/mL; Calbiochem, San Diego) was added to TEC subcultures to kill any remaining tumor cells.

### **Kinetic analysis and FUPI peptide distribution *in vivo***

LLC or B16 tumor-bearing mice were intravenously injected with 20 mg/kg Fitc-UPI (FUPI) peptide then sacrificed at different time points. Both tumor and non-tumor tissues were collected, fixed in 4% PFA and processed for immunofluorescence staining with anti-CD31 to visualize blood vessels. Images were captured by fluorescence microscopy using the green channel (FUPI), red channel (CD31) and blue channel (DAPI) simultaneously. FITC and CD31 fluorescent intensity was quantified using Metamorph software. The number of FUPI and CD31-positive vessels were counted and presented as a percentage of FUPI-positive vessels-to-total CD31-positive vessels.

### **Co-administration of anti-VEGF antibody or VEGFR2 kinase inhibitor and UPI peptide in LLC tumor model**

LLC tumor-bearing mice were intravenously injected with anti-VEGF antibody (B20-4.1.1) (1.5 mg/kg), UPI (10 mg/kg) or co-injected with anti-VEGF/UPI every-second-day for 12 days. Similarly, VEGFR2 kinase inhibitor was injected (0.5 mg/kg) or co-injected with inhibitor/UPI. Tumor growth was monitored as described above.

### ***In vivo* angiogenesis assays**

*In vivo* angiogenesis was analyzed using matrigel plugs and retina neovascularization as previously described (18, 51, 56, 57) with the following modifications: (1) *Matrigel Plug Angiogenesis Assay*: C56BL/6 mice were subcutaneously injected with 400  $\mu$ l phenol-free matrigel (BD Biosciences cat# 356231) containing 500 ng/ml VEGF and 100  $\mu$ g/ml UPI or CTR peptide. After 6 days, mice were sacrificed then the plugs were removed, fixed in 4% PFA and processed for immunofluorescence staining for CD31. (2) *Retina Neovascularization*: Wild type pups were intra-ocularly injected with 1  $\mu$ l of CTR or UPI peptide (1  $\mu$ g/ $\mu$ l) at postnatal day

(P)1, P3 and P5 as previously described (67). Pups were sacrificed at P6 then retinas were whole-mounted and stained with anti-isolectin B4 antibody as previously reported (51).

### **Hypoxia analysis in subcutaneous U87 glioma tumors**

Mice bearing subcutaneous U87 tumors were intraperitoneal injected with the hypoxia probe, pimonidazole hydrochloride (50 mg/ml stock solution; Hypoxyprobe, Inc, Burlington, MA), at 60 mg/kg body weight for 1 hour. Mice were then sacrificed and tumors fixed in 4% PFA. Hypoxia was measured by immunofluorescence staining of tumor samples. Areas of hypoxia were quantified using Image J software.

### ***In situ* VEGFR2 monitoring in the orthotopic U87 glioma model**

Control or UPI-peptide treated U87 glioma tumor-bearing mice were anesthetized with isofluorane, set up with a tail-vein catheter, put on a cradle, and inserted in a 7.0 Tesla small animal MRI system (Bruker Biospin). VEGFR2-targeted MRI probe (anti-VEGFR2-Gd-albumin-biotin) was administered as previously described (58). Pre- and 90 min post-contrast MRI images were taken following administration. Intensity of VEGFR2 was quantified using Image J software.

### **Biochemical pulldown assay using *ex vivo* tumors**

LLC tumors were homogenized in lysis buffer containing 50 mM Tris-HCl pH7.5, 150 mM NaCl, 0.05% NP-40, 10% Glycerol, 1x protease inhibitor cocktail (Calbiochem), and 20 mM NEM (*N-ethylmaleimide*). Protein concentration was determined by BCA kit (Pierce). Lysates ranging from 0.5-2 mg of protein were co-incubated with 100  $\mu$ M biotinylated UPI or CTR peptides, followed by the addition of Neutri-Avidin beads (Invitrogen) for pulldown binding assay. Beads were washed twice with lysis buffer, then twice with 1:1 lysis buffer:PBS. Beads

were then boiled for 5min in 2x sample loading buffer. Denatured proteins were subjected to Western blotting using anti-VEGFR2, anti-EGFR, anti-FGFR1 and anti-PDGFR- $\beta$  antibodies.

### **Construction and mammalian expression of human VEGFR2 kinase domain (KD)**

Human VEGFR2 kinase domain (KD) (59) was PCR-amplified from full length VEGFR2 template and cloned into TA cloning vector, pGEM-Teasy (Promega). Cloning was confirmed by sequencing (OMRF Core Facility). Resulting VEGFR2 KD with a 6xHis tag at the C-terminus was then inserted into mammalian expression vector, pcDNA3, by EcoRV/NotI sites. Resulting plasmid was transfected into 293T cells using Lipofectamine 2000. Twenty-four hours post-transfection, expression of His-tagged VEGFR2 KD was confirmed by Western blotting with anti-His antibody.

### **Construction and purification of recombinant VEGFR2 KD protein**

We used “BacPAK Baculovirus expression system” from Clontech Inc. In brief, the pGEM-Teasy-VEGFR2 KD-His created above was inserted into a transfer vector, pBacPAK8, by PstI/NotI restriction enzyme sites followed by *in vivo* recombination with BacPAK6 viral DNA in SF21 insect cells. Plaque selection and expression confirmation of VEGFR2 KD in SF21 insect cells were performed according to manufacturer’s instruction. Subsequent VEGFR2 purification was performed as previously reported (59-61). In brief, VEGFR2 KD was overexpressed in SF21 insect baculovirus expression system at high multiplicity. Three days after infection, cell pellets were lysed by dounce homogenization and short sonication in 20 mM Tris, pH8.0, 10 mM imidazole, 20 mM NaCl, 5% (v/v) glycerol, 1x protein inhibitors cocktail (Calbiochem) and 10 mM NEM. The lysate was centrifuged for 50 min at 35,000 rpm using a Ti90 rotor. The soluble fraction was loaded onto a Ni<sup>2+</sup> charged chelating sepharose (GE Healthcare) column. Before sample loading, the column was equilibrated with five column

volumes (CV) of cell lysis buffer. After sample loading, the column was washed with cell lysis buffer, then VEGFR2 KD was eluted with 20 mM Tris, pH8.0, 500 mM imidazole, 20 mM NaCl, 5% (v/v) glycerol and protein inhibitors cocktail (Calbiochem). VEGFR2 KD was pooled for sodium dodecyl sulfate polyacrylamide gel electrophoresis (SDS-PAGE) analysis. Pooled material was loaded onto a 6 mL anion exchanger Resource Q column (GE Healthcare) and washed extensively with 20 mM HEPES, pH8.0, 1 mM DTT, 1 mM EDTA. Protein was eluted using a 60 mL linear NaCl gradient in 20 mM HEPES, pH8.0, 500 mM NaCl, 1 mM DTT, 1 mM EDTA. Finally, VEGFR2 KD was purified by gel filtration on a Superdex 200 (GE Healthcare) column in 20 mM HEPES, pH7.5, 150 mM NaCl and 5% glycerol.

#### **SPR (Biacore) analysis of UPI-VEGFR2 binding affinity**

Binding of UPI or UPI-Mut (Q9A, A13S, and K16A) peptides to VEGFR2 KD were analyzed with surface plasmon resonance (SPR) in the Biacore 2000 biosensor (GE). CM5 biosensor chip flow cells were covalently coated with the recombinant VEGFR2 KD via standard amine coupling. The binding was analyzed in running buffer of 20 mM HEPES, pH7.5, 150 mM NaCl, and 5% glycerol. The kinetics of peptide interaction with VEGFR2 KD was determined by varying the ligand concentrations over a surface to which a specified concentration of receptors had been coupled. The contact time of peptides was 2 min and the flow rate was 5 ml/min. The flow cells were regenerated after every injection with 10 mM Glycine, pH1.7. The data were evaluated by subtracting the sensorgram obtained from the empty control flow cell from the sensorgram of the flow cells containing VEGFR2 KD. Assuming 1:1 binding, the dissociation constant was determined using SigmaPlot8.0 Software package.

#### **UIM peptide competition (Epsin 1-VEGFR2 interference) assay**

Epsin 1-HA (tag) and VEGFR2 KD-His(tag) were co-transfected into 293T cells using Lipofectamine 2000 (manufacturer's protocol). After 20 hours, cells were lysed in detergent-free hypotonic buffer (5 mM NaCl<sub>2</sub> in 10 mM HEPES, pH7.4) containing protease inhibitor cocktail (Roche) and 10 mM NEM. Cells were homogenized using a dounce homogenizer 10 times. Cell lysates were centrifuged at 13,000 rpm at 4°C for 10 min, and then the cleared supernatant collected. After incubating for 4 hours at 4°C with 300 μM peptide(s), supernatants were adjusted to isotonic condition by adding NaCl<sub>2</sub> up to 150 mM. Anti-His tag antibody (GenScript) was then added for immunoprecipitation (2 μg antibody in 200 μL lysates) at 4°C overnight. Immunocomplex was precipitated by addition of 30 μL rec-protein G beads (Invitrogen). Beads were washed 5 times in isotonic buffer with protease inhibitors. Samples were boiled for 5min using 2x sample loading buffer prior to Western blotting.

#### **UPI peptide binding to angiogenic receptors in HUVEC<sup>αvβ3</sup> by Biotin-ELISA assay**

Cultured HUVEC<sup>αvβ3</sup> cells were treated with angiogenic factor VEGF (or PDGF, EGF, FGF) and harvested. Cells were lysed in a buffer containing 25 mM Tris-HCl (pH 7.6), 150 mM NaCl, 0.25% NP-40 and 0.25% sodium deoxycholate with 1x protease inhibitors and 20 mM NEM. Two mg cell lysate was co-incubated with biotinylated UPI or CTR peptides with anti-VEGFR2 antibody (or anti-PDGFR-β, anti-EGFR, anti-FGFR1 antibody) and rec-G beads (invitrogen) for immunoprecipitation. Immunocomplexes were washed with lysis buffer then eluted using 50 μL of low pH elution buffer (0.1 M Glycine pH2.0) at room temperature for 10 min. Eluted supernatant was collected, followed by an addition of 1-3 μL of neutralization buffer (1 M Tris, pH 9.5) to balance the pH. The eluted samples were subjected to biotin-ELISA analysis (MyBioSource). Background was subtracted from a basal sample (without adding peptide).

#### **Bioinformatic analysis of UPI peptides and putative binding with VEGFR2**

(1) *Molecular Dynamics Simulation*: Three-dimensional (3D) structures of UIM and UPI were predicted by PEP-FOLD (<http://bioserv.rpbs.univ-paris-diderot.fr/PEP-FOLD>) (62, 63). Models were clustered by the sOPEP energy value (the coarse grained energy), then ranked based on their cluster scores. The top 5 clusters were used for the proposed native and near-native conformations. PEP-FOLD yielded a predicted model with an average root mean square deviation (RMSD) of 2.1 Å based on NMR structure (63). (2) *Molecular Docking Procedure*: Docking experiments were performed using ClusPro program (64, 65). 3D crystal structures of ubiquitin (PDB ID: 1UBQ) and VEGFR2 kinase domain (PDB ID: 3U6J) were obtained from NCBI Protein Database. Apo-open crystal structure of VEGFR2 kinase domain was obtained by removing pyrazolone, the co-crystallized VEGFR2 kinase inhibitor, from its binding site. Simulated models of UIM and UPI peptide were then docked into ubiquitin or VEGFR2 kinase domain independently to generate predicted binding models of UIM-Ub, UPI-Ub, UIM-VEGFR2 and UPI-VEGFR2. The obtained UPI-Ub model with the high scores and best topologies was further docked into VEGFR2 kinase domain to generate the model of UPI-Ub-VEGFR2 super complex.

### **Standard and previously published methodologies**

Western blotting, H&E staining, immunofluorescence staining, confocal microscopy, transmission electron microscopy (TEM) and cell culture maintenance were performed according to standard methodologies. Confocal and fluorescent microscopy images were captured using an Olympus IX81 Spinning Disc Confocal Microscope with an Olympus plan Apo Chromat 60x objective and Hamamatsu Orca-R<sup>2</sup> Monochrome Digital Camera C1D600. **Site-directed mutagenesis was performed using QuikChange II XL Site-Directed Mutagenesis Kit** (Agilent Technologies, Inc) and confirmed by DNA sequencing (OMRF Sequencing

**Facility). HUVEC transfection, FACS analysis, *in vitro* angiogenesis assays, VEGF signaling and VEGFR2 internalization assays were performed** as previously described (17, 18, 54). *In vivo* FITC-dextran perfusion assays to evaluate vessel function were performed as previously described (17, 68).

### **Statistical analysis**

Data were presented as the mean  $\pm$  SEM. Data were analyzed by a two-tailed student's *t* test or ANOVA with Bonferron's procedure for multiple comparisons. A *p* value of less than 0.05 was considered statistically significant.

## Supplemental Figure Legends

### Supplemental Figure 1. UPI peptide pharmacokinetics in endothelial cells and in tumor vasculature, and its action on VEGFR2 endocytosis, related to Figure 1.

(A) HUVECs were co-transfected with integrins  $\alpha v$  and  $\beta 3$  plasmids by electroporation, generating HUVEC <sup>$\alpha v\beta 3$</sup>  cells. 10  $\mu$ M FUPI (FITC-conjugated UPI) peptide was added to HUVEC <sup>$\alpha v\beta 3$</sup>  cells or pcDNA transfected control HUVECs. Expression of  $\alpha v\beta 3$  was measured by Western blot; n=3.

(B) Different concentration of FUPI was added to HUVEC <sup>$\alpha v\beta 3$</sup>  cells. FITC was recorded by fluorescent microscopy at different time points as indicated, n=4.

(C) Quantification of (B), \*, \*\* P<0.05. Scale bar: 100 $\mu$ m.

(D) FUPI peptide was targeted to plasma membrane via Lyn PM anchoring sequence in HUVEC <sup>$\alpha v\beta 3$</sup>  cells revealed by confocal microscopy. Scale bar: 10 $\mu$ m.

(E) FUPI peptide (10mg/kg, one injection) was i.v.-injected into mice bearing B16 tumors. A time course was scheduled to sacrifice mice as indicated from 2-48 hrs. Pharmacokinetics was analyzed as shown. Scale bar: 100 $\mu$ m.

(F) UPI peptide treatment blocked Epsin 1-VEGFR2 interaction in endogenous HUVEC <sup>$\alpha v\beta 3$</sup> . Cells were treated with 50ng/ml VEGF for 5min, followed by lysis of cells, immunoprecipitation and Western blotting analysis using specific VEGFR2 or Epsin 1 (Epn1) antibodies; n=5; \*P<0.001.

(G) UPI peptide increases VEGFR2 retention on the PM of HUVEC <sup>$\alpha v\beta 3$</sup>  cells revealed by FACS analysis, n=3.

(H) Quantification of (G); n=3, \*P<0.05.

(I) UPI peptide disabled VEGFR2 endocytosis measured by biotin-labeled-VEGF internalization in HUVEC<sup>αvβ3</sup> cells visualized by confocal microscopy, n=5. As shown, after incubation at 37°C, in the UPI peptide-treated cells, VEGFR2 endocytosis was minimal; Scale bar: 10μm.

**Supplemental Figure 2. FUPI specifically targets to tumors only and inhibits tumor growth, related to Figure 1 and 2.**

(A) B16 tumor bearing mice were sacrificed at 24-hr time point after control (PBS) or FUPI peptide injection (10mg/kg, i.v.-injection). Tumor and major organs were stained with CD31 (red) and imaged using the red channel (CD31), blue channel (DAPI) and green channel (FUPI). Note that the yellowish color (red/green merge) is seen only in tumors; other major organs (liver, lung, heart, spleen, kidney, colon and brain, etc) are free of green color; n=4. Scale bar: 200μm.

(B) Control (CTR) or UPI peptide was i.p.-injected (20mg/kg, every-other-day) from 20-35 weeks in normal and TRAMP animal models. Representative images of H&E stained normal prostate, TRAMP prostate and TRAMP-UPI prostate, n=18. Images show reduced tumors after UPI treatment; Scale bar: 100μm.

(C) Comparison of therapeutic efficacy among AP-UIM, UI, UPI and CTR peptides in LLC tumor models, n>5; P values are indicated in the figure.

**Supplemental Figure 3. UPI peptide is a specific VEGFR2 modifier but does not affect other major angiogenic factor signaling pathways *in vitro* or in tumors, related to Figure 4.**

(A-B) Anti-VEGF antibody neutralizes VEGF/UPI peptide-mediated augmentation of VEGFR2 signaling. HUVEC<sup>αvβ3</sup> cells were pretreated with 10μM control (CTR) or UPI peptide for 15 hours. Cells were then starved for 3 hours, followed by pre-treatment with anti-VEGF antibody (200μg/ml) for 1 hour and then stimulated by VEGF (50ng/ml) for 5min. Cell lysates were subjected to Western blotting using antibodies as indicated in (A).

(B) Quantification of P-VEGFR2 from (A), n=4; P value of statistical analysis is indicated in the figure.

(C) Binding affinity of biotinylated-UPI peptide to VEGFR2, FGFR1 PDGFR- $\beta$  and EGFR determined by binding affinity-ELISA assay in HUVEC $^{\alpha v\beta 3}$  cells. Note that UPI peptide did not interact with FGFR1, PDGFR- $\beta$  or EGFR, n=5; \*P<0.001; n.s: no statistical difference.

(D-F) Quantifications of phosphorylated PLC- $\gamma$ , AKT and ERK relative to total under different stimulations in Fig. 3D.

(G) Western blotting analysis of VEGFR2, EGFR1, TGF $\beta$ 1 and PDGFR- $\beta$  in representative CTR or UPI peptide-treated B16 melanoma tumors.

(H) Quantification of protein expression in (G), n =5; \*P<0.05.

(I) Expression of angiogenic receptors and P-VEGFR2 in CTR or UPI peptide-treated U87 glioma mouse tumors.

(J-K) UPI peptide treatment did not change the expression of epsin 1 (Epn1) and epsin 2 (Epn2) in HUVEC $^{\alpha v\beta 3}$  cells or U87 glioma tumors, n=5.

**Supplemental Figure 4. UPI peptide does not affect VEGFR1, VEGFR3 or Notch signaling in endothelial cells, related to Figure 4.**

(A) HUVEC $^{\alpha v\beta 3}$  cells were treated with UPI or control (CTR) peptides. Prior to lysis, cells were stimulated with VEGF for 5 min. Lysates were analyzed by Western blotting using anti-VEGFR1 and VEGFR3 antibodies;

(B) HUVEC $^{\alpha v\beta 3}$  cells were treated as in (A) then lysates were immunoprecipitated with anti-VEGFR1 antibody and phosphorylation analyzed by Western blotting using 4G10 antibody;

(C) Mouse primary ECs (MEC) were isolated, cultured, and co-transfected with plasmids of  $\alpha v$  and  $\beta 3$ , pre-treated with 10 $\mu$ M DAPT ( $\gamma$ -secretase inhibitor) or DMSO (vehicle) for 24 hrs, and

then treated with UPI or CTR peptides at 25 $\mu$ M for an additional 16 hrs. Cell lysates were analyzed by Western blotting using anti-NICD and Dll4 antibodies;

(D) Quantification of NICD expression in (C), n=4. n.s, no statistical difference.

**Supplemental Figure 5a. Strategy for generating genetically modified animal models, related to Figure 5.**

Mice were crossed as shown to establish genetically modified animal models. Genotyping and selection of mice for breeding are routinely performed using standard procedures.

(A) Flk-1<sup>+/-</sup>; (B) EC-iDKO; (C) EC-iDKO-Flk-1<sup>+/-</sup>; (D) EC-iDKO-Notch.

**Supplemental Figure 5b. UPI peptide therapeutic concept and targeting specificity in genetically modified mice harboring a loss in VEGFR2 allele, related to Figure 5.**

Therapeutic efficacy of UPI peptide is predicted to be dependent on the expression level of VEGFR2 *in vivo* (Flk-1<sup>+/-</sup>); Less VEGFR2 normalizes UPI peptide effect on tumor angiogenesis.

**Supplemental Figure 5c. UPI peptide therapeutic concept and targeting specificity in genetically modified mice harboring epsin deficiency and a loss in VEGFR2 allele, related to Figure 5.**

Therapeutic efficacy of UPI peptide is predicted to be dependent on the expression level of epsins *in vivo* (EC-iDKO or EC-iDKO-Flk-1<sup>+/-</sup>); Loss of epsins impairs UPI peptide effect on tumor angiogenesis.

**Supplemental Figure 6. UPI peptide treatment augments tumor angiogenesis revealed by immunostaining using Ve-cadherin antibody in LLC and U87 tumor models, related to Figure 7.**

(A). Representative images of immunofluorescent staining using anti-Ve-Cadherin antibody; n=5 in each group; scale bar: 200 $\mu$ m.

(B). Fold change of vessel density; CTR vs. UPI, \* P<0.001;

(C). Diameter of vessel. n=5. CTR vs. UPI; # P<0.001.

**Supplemental Figure 7. UPI peptide increases tumor vessel permeability and leakage, but does not cause vessel leakage in other major organs (non-tumor organs), related to Figure 7.**

(A-F) Quantifications for Figure 6D (VEGFR2), 6E (P-VEGFR2), 6F (vessel permeability), 6G ( $\alpha$ -SMA coverage), 6I (tumor hypoxia) and 6J (% of perfused vessel in intestine), respectively; n>5.

(G) Tumors collected from UPI peptide treated U87/SCID animal models were prepared for TEM analysis. (a) Representative image of UPI peptide treated U87 tumor depicting fenestration in the endothelium; indicated by black arrows; (b) Representative image of UPI peptide treated U87 tumor showing platelet aggregations in an open junction (red double arrow) between two ECs. RBC: red blood cell; P: platelet; EC: endothelial cells; (c) Representative image taken from U87 control tumor, showing red blood cells are inside vessels; (d) Representative image of UPI peptide treated U87 tumor showing increased permeability and significant RBC leakage in semi-thin sections (red arrowheads); n=5 for all data; Scale bar (a, b): 500nm; (c, d): 100 $\mu$ m.

(H) B16-melanoma tumor bearing mice were i.v.-injected with control or UPI peptides for 16 days (dosage: 10mg/kg, every-other-day). Mice were perfused with FITC-Dextran injection for 10min. Tumors and other major organs were harvested and fixed for CD31 staining. FITC (green) and CD31 (red) were visualized simultaneously by confocal microscopy. Data showing no leakage in all examined non-tumor organs; n=3; Scale bar: 100 $\mu$ m.

(I) Mice were i.v.-injected with different dosage of UPI peptides for 3 months and blood serums were subjected to biochemical test by UT Southwestern service facility at Dallas, TX; n=5.

**Supplemental Figure 8. UPI peptide has increased efficacy when combined with cytotoxic chemotherapeutics; related to Figure 7.**

(A) Representative images of tumors from subcutaneous LLC tumor-bearing mice treated with anti-VEGF/Dox, UPI/Dox, anti-VEGF/Taxol or UPI/Taxol, n=6; Scale Bar: 4mm.

(B) Representative TUNEL Staining of LLC tumors shown in (A), n=6; Scale bar: 100 $\mu$ m.

(C-D) Quantification (C) and representative images (D) of orthotopic GL261 tumor-bearing mice treated with UPI/OKN versus anti-VEGF/OKN. Dosages used: intravenous injection of 5 mg/kg UPI or 2.5 mg/kg anti-VEGF antibody every-second-day, and 0.1% OKN-007 (w/v or 75 mg/kg/day) in drinking water. n=5; P<0.05. Data is taken at post-implantation Day-23.

**Supplemental Table**

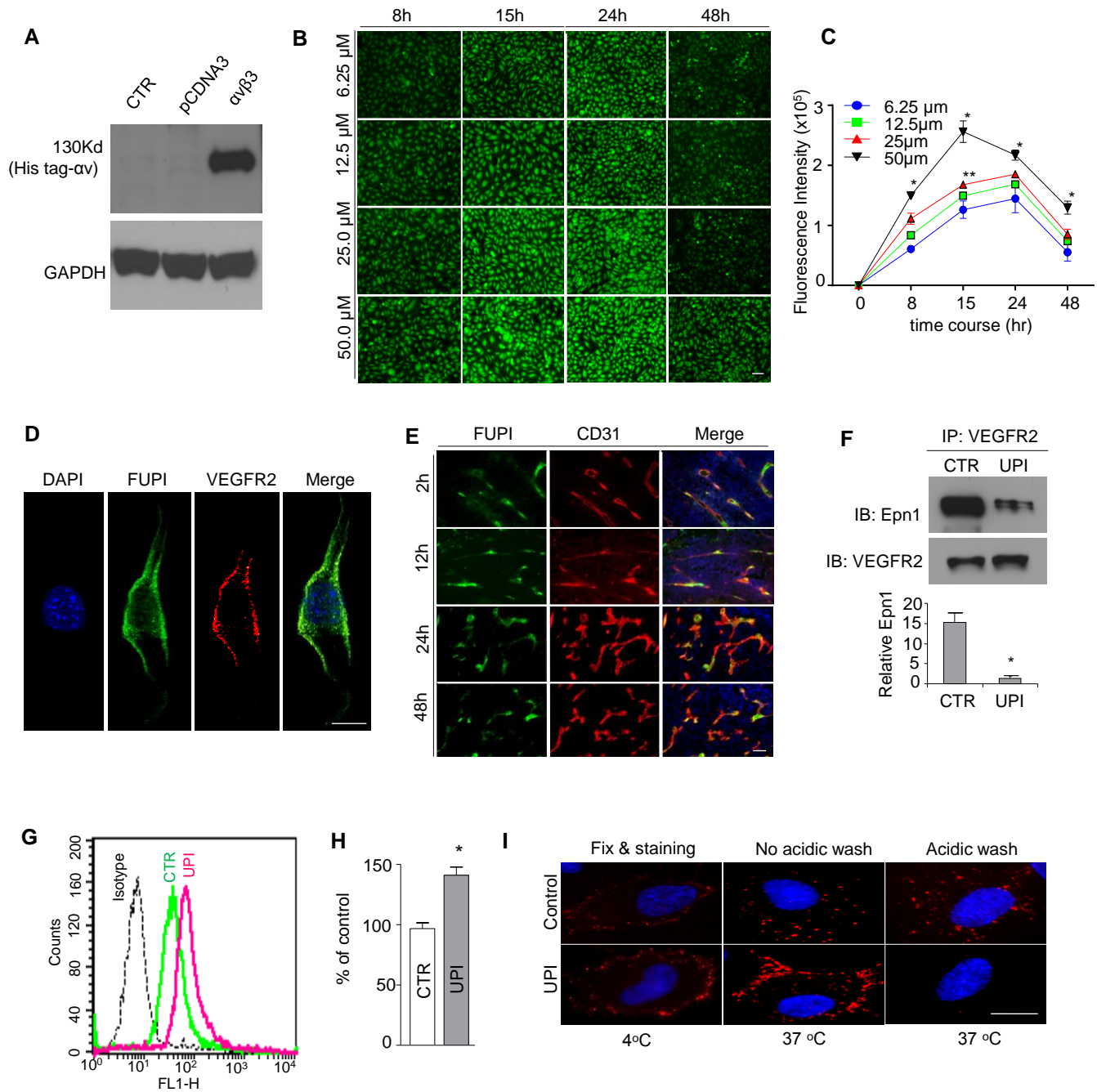
**Supplemental Table 1:** Peptides used in this study (Related to all Figures)

**Supplemental References**

1. Pasula, S., Cai, X., Dong, Y., Messa, M., McManus, J., Chang, B., Liu, X., Zhu, H., Mansat, R.S., Yoon, S.J., et al. 2012. Endothelial epsin deficiency decreases tumor growth by enhancing VEGF signaling. *J Clin Invest* 122:4424-4438.
2. Rosenthal, J.A., Chen, H., Slepnev, V.I., Pellegrini, L., Salcini, A.E., Di Fiore, P.P., and De Camilli, P. 1999. The epsins define a family of proteins that interact with components of the clathrin coat and contain a new protein module. *J Biol Chem* 274:33959-33965.
3. Tessneer, K.L., Pasula, S., Cai, X., Dong, Y., McManus, J., Liu, X., Yu, L., Hahn, S., Chang, B., Chen, Y., et al. 2014. Genetic reduction of vascular endothelial growth factor receptor 2 rescues aberrant angiogenesis caused by epsin deficiency. *Arterioscler Thromb Vasc Biol* 34:331-337.
4. Tessneer, K.L., Pasula, S., Cai, X., Dong, Y., Liu, X., Yu, L., Hahn, S., McManus, J., Chen, Y., Chang, B., et al. 2013. Endocytic Adaptor Protein Epsin Is Elevated in Prostate Cancer and Required for Cancer Progression. *ISRN Oncology* 2013:8.
5. Doblas, S., He, T., Saunders, D., Hoyle, J., Smith, N., Pye, Q., Lerner, M., Jensen, R.L., and Towner, R.A. 2012. In vivo characterization of several rodent glioma models by 1H MRS. *NMR Biomed* 25:685-694.

6. Towner, R.A., Gillespie, D.L., Schwager, A., Saunders, D.G., Smith, N., Njoku, C.E., Krysiak, R.S., 3rd, Larabee, C., Iqbal, H., Floyd, R.A., et al. 2013. Regression of glioma tumor growth in F98 and U87 rat glioma models by the Nitron OKN-007. *Neuro-oncology* 15:330-340.
7. Liu, Z., Kobayashi, K., van Dinther, M., van Heiningen, S.H., Valdimarsdottir, G., van Laar, T., Scharpfenecker, M., Lowik, C.W., Goumans, M.J., Ten Dijke, P., et al. 2009. VEGF and inhibitors of TGFbeta type-I receptor kinase synergistically promote blood-vessel formation by inducing alpha5-integrin expression. *J Cell Sci* 122:3294-3302.
8. Valapala, M., Thamake, S.I., and Vishwanatha, J.K. 2011. A competitive hexapeptide inhibitor of annexin A2 prevents hypoxia-induced angiogenic events. *J Cell Sci* 124:1453-1464.
9. Nakayama, M., Nakayama, A., van Lessen, M., Yamamoto, H., Hoffmann, S., Drexler, H.C., Itoh, N., Hirose, T., Breier, G., Vestweber, D., et al. 2013. Spatial regulation of VEGF receptor endocytosis in angiogenesis. *Nat Cell Biol* 15:249-260.
10. Cai, X., Sezate, S.A., Seal, S., and McGinnis, J.F. 2012. Sustained protection against photoreceptor degeneration in tubby mice by intravitreal injection of nanoceria. *Biomaterials* 33:8771-8781.
11. He, T., Smith, N., Saunders, D., Pittman, B.P., Lerner, M., Lightfoot, S., Silasi-Mansat, R., Lupu, F., and Towner, R.A. 2013. Molecular MRI differentiation of VEGF receptor-2 levels in C6 and RG2 glioma models. *Am J Nucl Med Mol Imaging* 3:300-311.
12. McTigue, M., Murray, B.W., Chen, J.H., Deng, Y.L., Solowiej, J., and Kania, R.S. 2012. Molecular conformations, interactions, and properties associated with drug efficiency and clinical performance among VEGFR TK inhibitors. *Proc Natl Acad Sci U S A* 109:18281-18289.
13. Leppanen, V.M., Jeltsch, M., Anisimov, A., Tvorogov, D., Aho, K., Kalkkinen, N., Toivanen, P., Yla-Herttuala, S., Ballmer-Hofer, K., and Alitalo, K. 2011. Structural determinants of vascular endothelial growth factor-D receptor binding and specificity. *Blood* 117:1507-1515.
14. Leppanen, V.M., Prota, A.E., Jeltsch, M., Anisimov, A., Kalkkinen, N., Strandin, T., Lankinen, H., Goldman, A., Ballmer-Hofer, K., and Alitalo, K. 2010. Structural determinants of growth factor binding and specificity by VEGF receptor 2. *Proc Natl Acad Sci U S A* 107:2425-2430.
15. Maupetit, J., Derreumaux, P., and Tuffery, P. 2009. PEP-FOLD: an online resource for de novo peptide structure prediction. *Nucleic Acids Res* 37:W498-503.
16. Thevenet, P., Shen, Y., Maupetit, J., Guyon, F., Derreumaux, P., and Tuffery, P. 2012. PEP-FOLD: an updated de novo structure prediction server for both linear and disulfide bonded cyclic peptides. *Nucleic Acids Res* 40:W288-293.
17. Comeau, S.R., Gatchell, D.W., Vajda, S., and Camacho, C.J. 2004. ClusPro: a fully automated algorithm for protein-protein docking. *Nucleic Acids Res* 32:W96-99.
18. Comeau, S.R., Gatchell, D.W., Vajda, S., and Camacho, C.J. 2004. ClusPro: an automated docking and discrimination method for the prediction of protein complexes. *Bioinformatics* 20:45-50.
19. Liu, X., Pasula, S., Song, H., Tessneer, K. L., Dong, Y., Hahn, S., Tadayuki, Y., Brophy, M. L., Chang, B., Cai, X., Wu, H., McManus, J., Ichise, H., Georgescu, C., Wren, J. D., Griffin, C., Xia, L., Srinivasan, R. S., Chen, H. 2014. Temporal and spatial regulation of

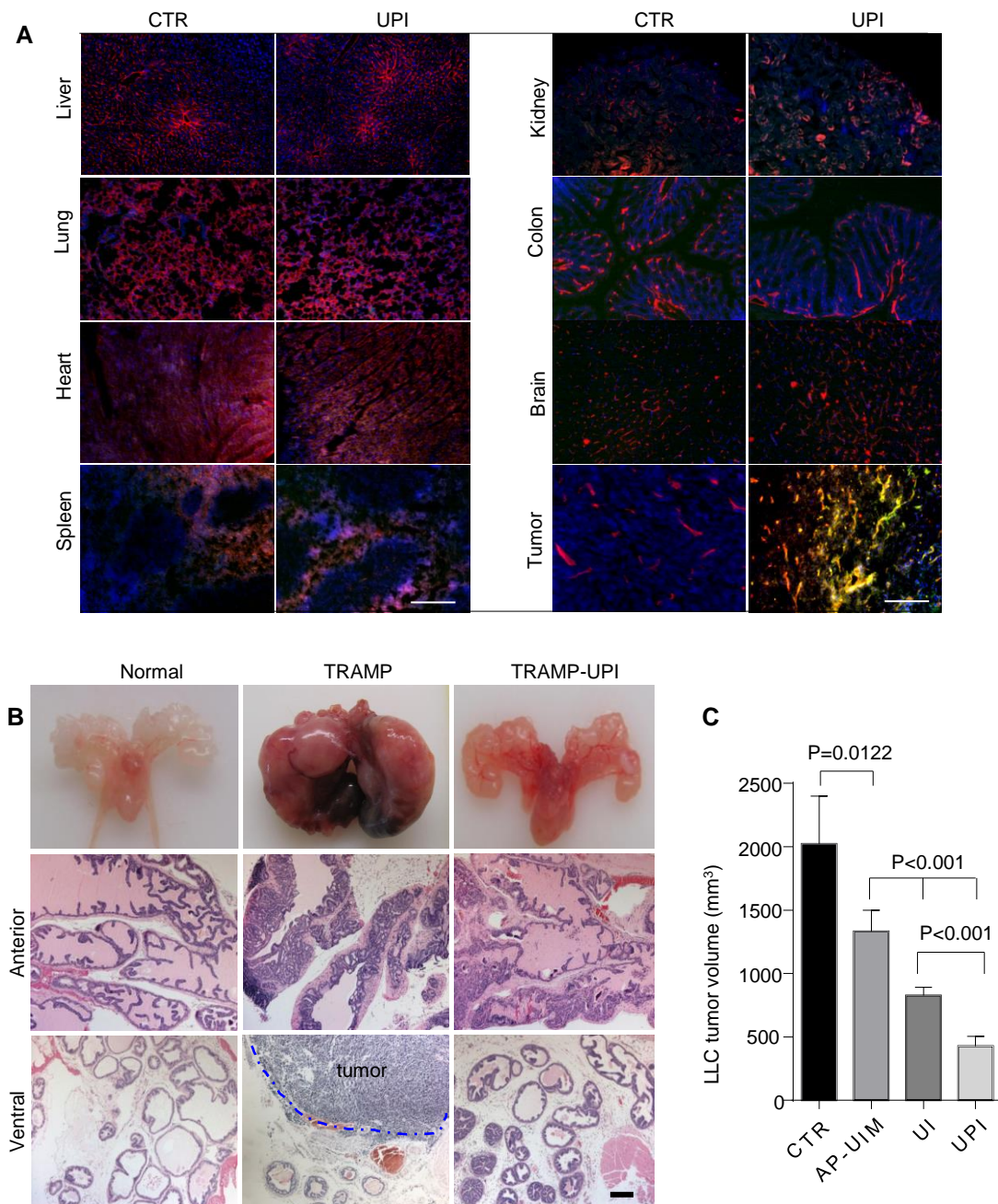
epsin abundance and VEGFR3 signaling are required for lymphatic valve formation and function. *Science Signaling* 7.



**Supplemental Figure 1. UPI peptide pharmacokinetics in endothelial cells and in tumor vasculature, and its action on VEGFR2 endocytosis, related to Figure 1.**

**Supplemental Figure 1. UPI peptide pharmacokinetics in endothelial cells and in tumor vasculature, and its action on VEGFR2 endocytosis, related to Figure 1.**

- (A) HUVECs were co-transfected with integrins  $\alpha v$  and  $\beta 3$  plasmids by electroporation, generating HUVEC $^{\alpha v\beta 3}$  cells. 10  $\mu$ M FUPI (FITC-conjugated UPI) peptide was added to HUVEC $^{\alpha v\beta 3}$  cells or pcDNA transfected control HUVECs. Expression of  $\alpha v\beta 3$  was measured by Western blot; n=3.
- (B) Different concentration of FUPI was added to HUVEC $^{\alpha v\beta 3}$  cells. FITC was recorded by fluorescent microscopy at different time points as indicated, n=4.
- (C) Quantification of (B), \*, \*\* P<0.05. Scale bar: 100 $\mu$ m.
- (D) FUPI peptide was targeted to plasma membrane via Lyn PM anchoring sequence in HUVEC $^{\alpha v\beta 3}$  cells revealed by confocal microscopy. Scale bar: 10 $\mu$ m.
- (E) FUPI peptide (10mg/kg, one injection) was i.v.-injected into mice bearing B16 tumors. A time course was scheduled to sacrifice mice as indicated from 2-48 hrs. Pharmacokinetics was analyzed as shown. Scale bar: 100 $\mu$ m.
- (F) UPI peptide treatment blocked Epsin 1-VEGFR2 interaction in endogenous HUVEC $^{\alpha v\beta 3}$ . Cells were treated with 50ng/ml VEGF for 5min, followed by lysis of cells, immunoprecipitation and Western blotting analysis using specific VEGFR2 or Epsin 1 (Epn1) antibodies; n=5; \*P<0.001.
- (G) UPI peptide increases VEGFR2 retention on the PM of HUVEC $^{\alpha v\beta 3}$  cells revealed by FACS analysis, n=3.
- (H) Quantification of (G); n=3, \*P<0.05.
- (I) UPI peptide disabled VEGFR2 endocytosis measured by biotin-labeled-VEGF internalization in HUVEC $^{\alpha v\beta 3}$  cells visualized by confocal microscopy, n=5. As shown, after incubation at 37° C, in the UPI peptide-treated cells, VEGFR2 endocytosis was minimal; Scale bar: 10 $\mu$ m.

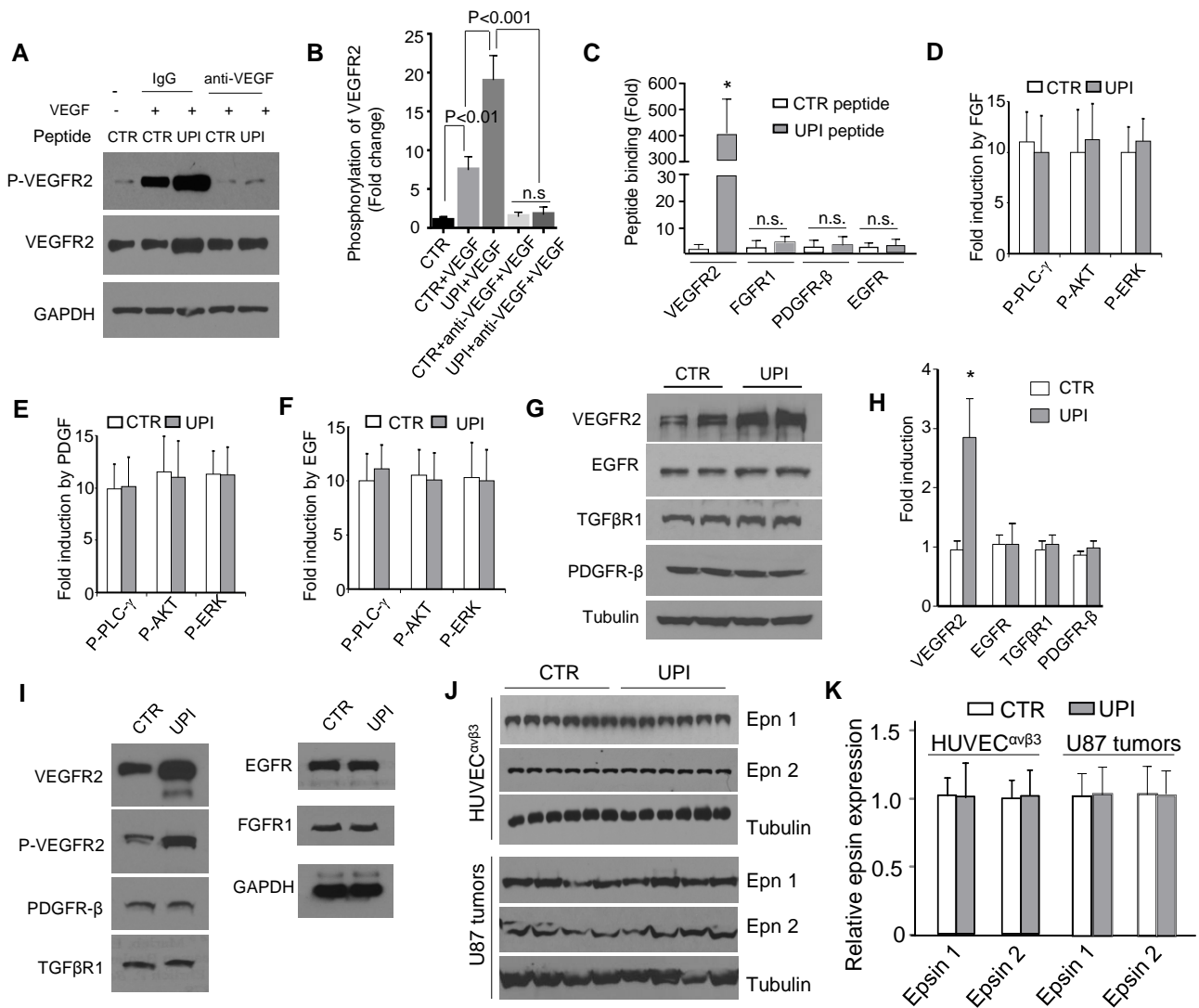


**Supplemental Figure 2. FUPI specifically targets to tumors only and inhibits tumor growth, related to Figure 2.**

(A) B16 tumor bearing mice were sacrificed at 24-hr time point after control (PBS) or FUPI peptide injection (10mg/kg, i.v.-injection). Tumor and major organs were stained with CD31 (red) and imaged using the red channel (CD31), blue channel (DAPI) and green channel (FUPI). Note that the yellowish color (red/green merge) is seen only in tumors; other major organs (liver, lung, heart, spleen, kidney, colon and brain, etc) are free of green color; n=4. Scale bar: 200 $\mu$ m.

(B) Control (CTR) or UPI peptide was i.p.-injected (20mg/kg, every-other-day) from 20-35 weeks in normal and TRAMP animal models. Representative images of H&E stained normal prostate, TRAMP prostate and TRAMP-UPI prostate, n=18. Images show reduced tumors after UPI treatment; Scale bar: 100 $\mu$ m.

(C) Comparison of therapeutic efficacy among AP-UIM, UI, UPI and CTR peptides in LLC tumor models, n>5; P values are indicated in the figure.



**Supplemental Figure 3. UPI peptide is a specific VEGFR2 modifier but does not affect other major angiogenic factor signaling pathways *in vitro* or in tumors, related to Figure 4.**

(A-B) Anti-VEGF antibody neutralizes VEGF/UPI peptide-mediated augmentation of VEGFR2 signaling. HUVEC<sup>avβ3</sup> cells were pretreated with 10μM control (CTR) or UPI peptide for 15 hours. Cells were then starved for 3 hours, followed by pre-treatment with anti-VEGF antibody (200μg/ml) for 1 hour and then stimulated by VEGF (50ng/ml) for 5min. Cell lysates were subjected to Western blotting using antibodies as indicated in (A).

(B) Quantification of P-VEGFR2 from (A), n=4; P value of statistical analysis is indicated in the figure.

(C) Binding affinity of biotinylated-UPI peptide to VEGFR2, FGFR1 PDGFR-β and EGFR determined by binding affinity-ELISA assay in HUVEC<sup>avβ3</sup> cells. Note that UPI peptide did not interact with FGFR1, PDGFR-β or EGFR, n=5; \*P<0.001; n.s: no statistical difference.

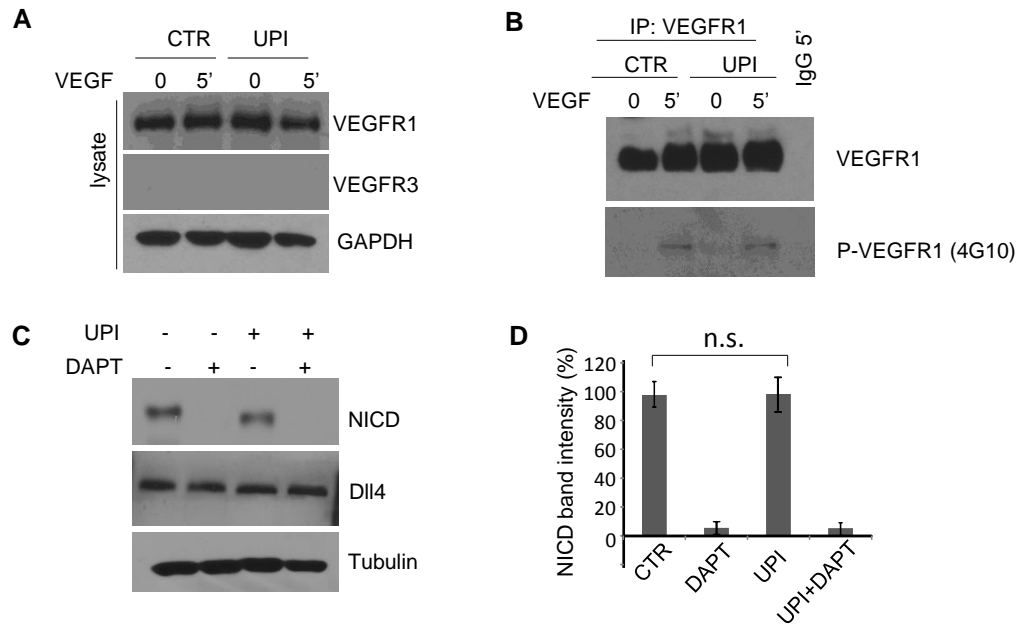
(D-F) Quantifications of phosphorylated PLC-γ, AKT and ERK relative to total under different stimulations in Fig. 3D.

(G) Western blotting analysis of VEGFR2, EGFR1, TGFβR1 and PDGFR-β in representative CTR or UPI peptide-treated B16 melanoma tumors.

(H) Quantification of protein expression in (G), n =5; \*P<0.05.

(I) Expression of angiogenic receptors and P-VEGFR2 in CTR or UPI peptide-treated U87 glioma mouse tumors.

(J-K) UPI peptide treatment did not change the expression of epsin 1 (Epn1) and epsin 2 (Epn2) in HUVEC<sup>avβ3</sup> cells or U87 glioma tumors, n=5.



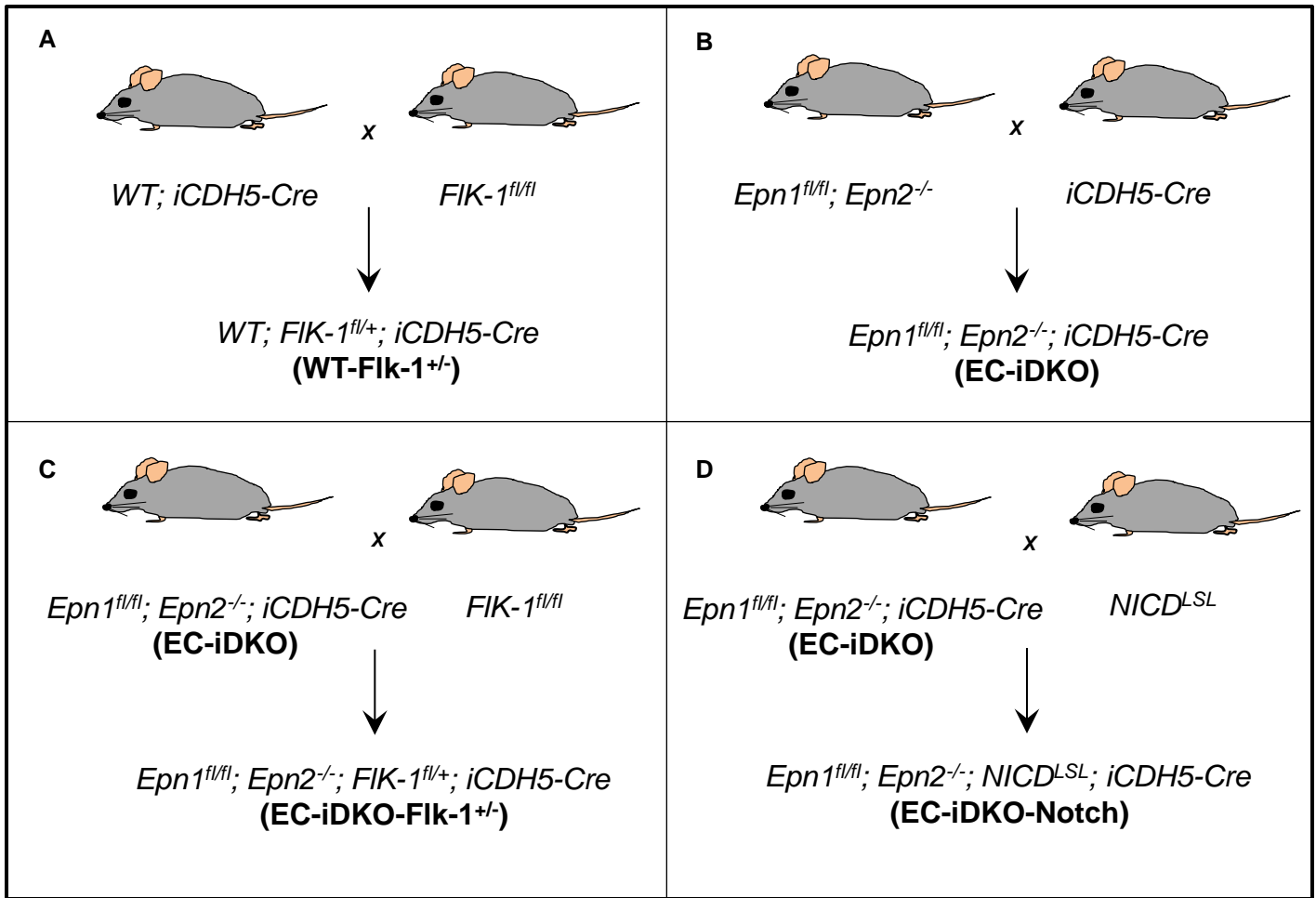
**Supplemental Figure 4. UPI peptide does not affect VEGFR1, VEGFR3 or Notch signaling in endothelial cells, related to Figure 4.**

(A) HUVEC $\alpha\beta^3$  cells were treated with UPI or control (CTR) peptides. Prior to lysis, cells were stimulated with VEGF for 5 min. Lysates were analyzed by Western blotting using anti-VEGFR1 and VEGFR3 antibodies;

(B) HUVEC $\alpha\beta^3$  cells were treated as in (A) then lysates were immunoprecipitated with anti-VEGFR1 antibody and phosphorylation analyzed by Western blotting using 4G10 antibody;

(C) Mouse primary ECs (MEC) were isolated, cultured, and co-transfected with plasmids of  $\alpha$  and  $\beta$ 3, pre-treated with 10 $\mu$ M DAPT ( $\gamma$ -secretase inhibitor) or DMSO (vehicle) for 24 hrs, and then treated with UPI or CTR peptides at 25 $\mu$ M for an additional 16 hrs. Cell lysates were analyzed by Western blotting using anti-NICD and DII4 antibodies;

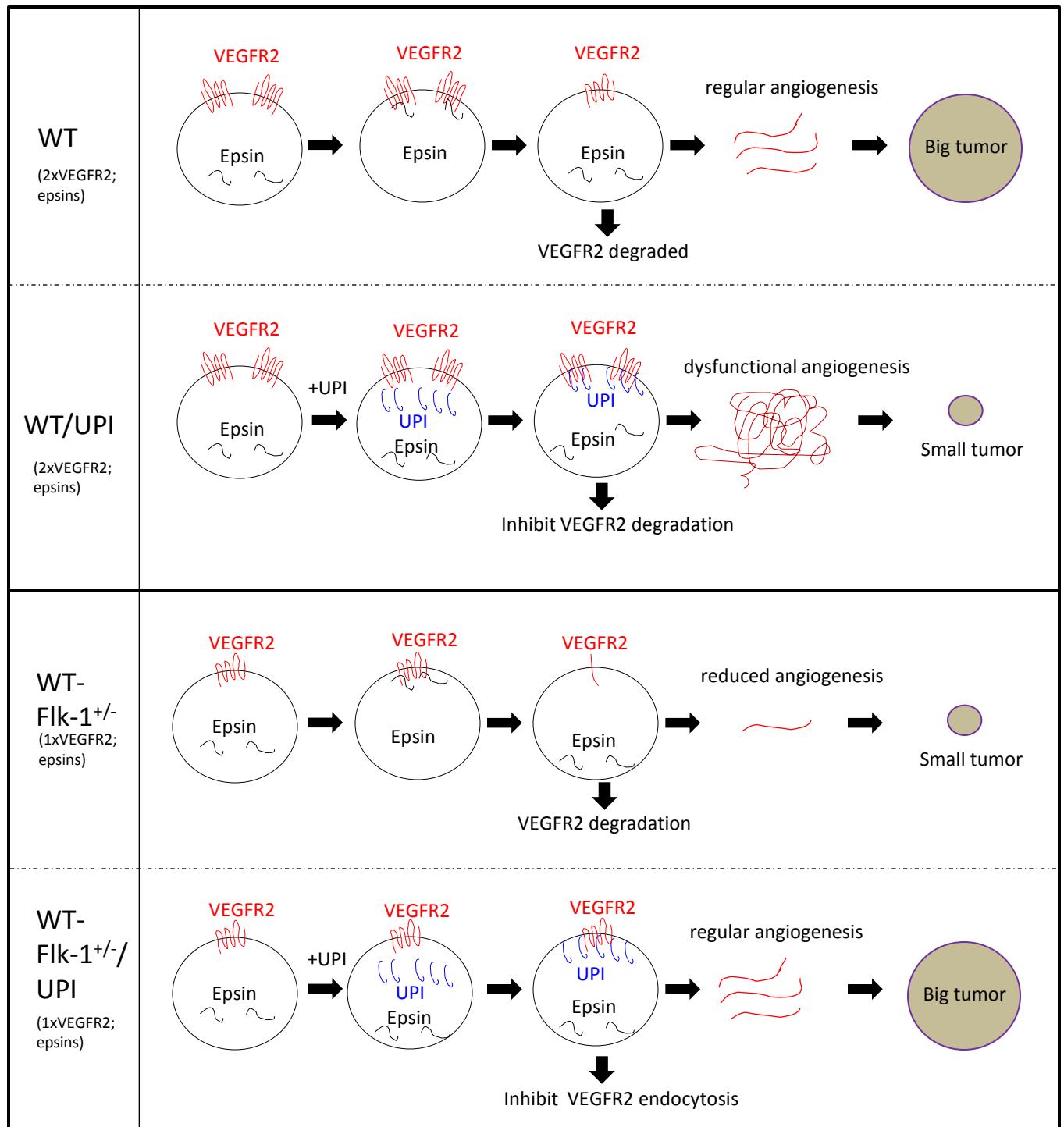
(D) Quantification of NICD expression in (C), n=4. n.s., no statistical difference.



**Supplemental Figure 5a. Strategy for generating genetically modified animal models, related to Figure 5.**

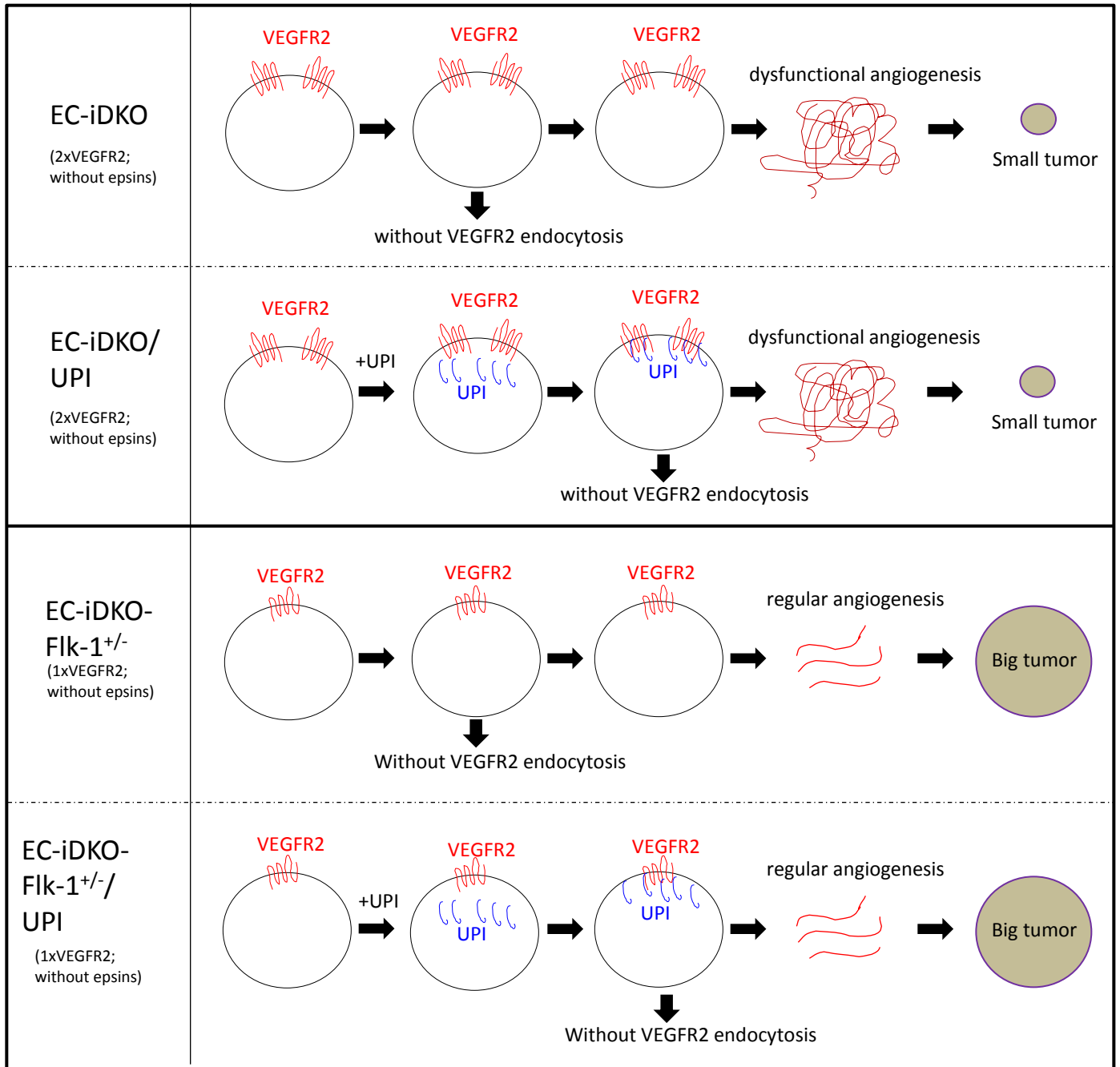
Mice were crossed as shown to establish genetically modified animal models. Genotyping and selection of mice for breeding are routinely performed using standard procedures.

(A) *Flk-1<sup>+/-</sup>*; (B) EC-iDKO; (C) EC-iDKO-*Flk-1<sup>+/-</sup>*; (D) EC-iDKO-Notch.



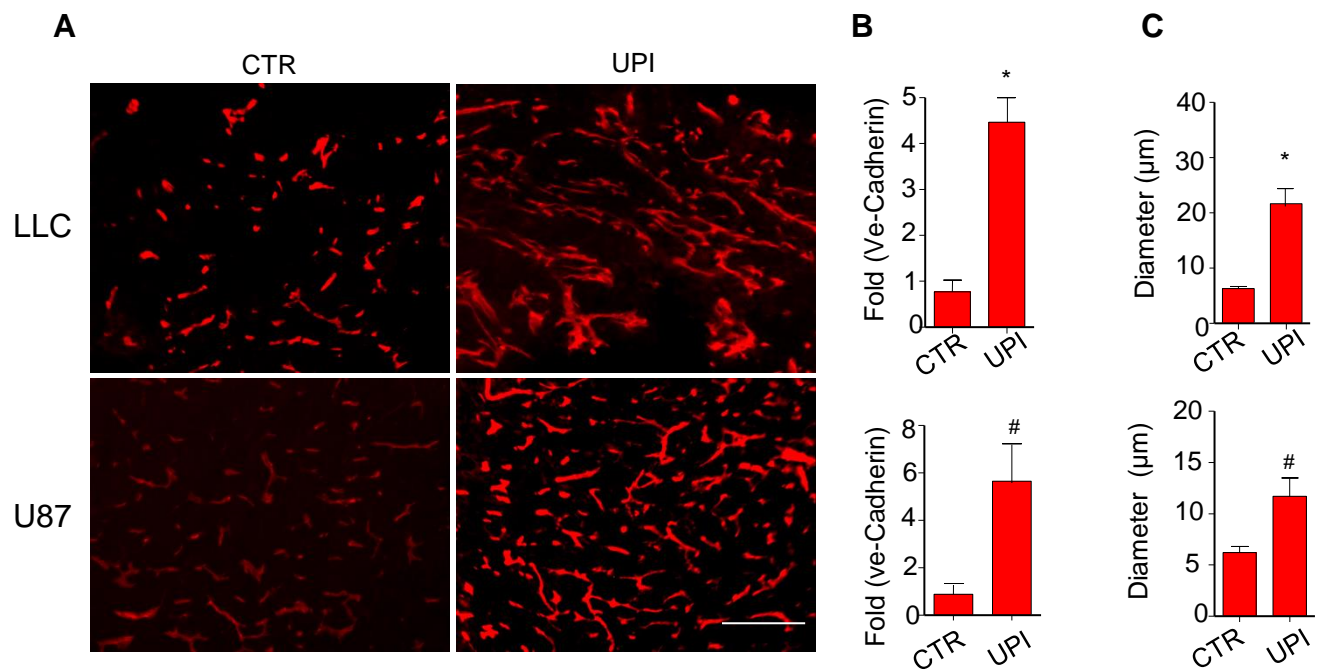
**Supplemental Figure 5b. UPI peptide therapeutic concept and targeting specificity in genetically modified mice harboring a loss in VEGFR2 allele, related to Figure 5.**

Therapeutic efficacy of UPI peptide is predicted to be dependent on the expression level of VEGFR2 *in vivo* (Flk-1<sup>+/-</sup>); Less VEGFR2 normalizes UPI peptide effect on tumor angiogenesis.



**Supplemental Figure 5c. UPI peptide therapeutic concept and targeting specificity in genetically modified mice harboring epsin deficiency and a loss in VEGFR2 allele, related to Figure 5.**

Therapeutic efficacy of UPI peptide is predicted to be dependent on the expression level of epsins *in vivo* (EC-iDKO or EC-iDKO-Flk-1<sup>+/-</sup>); Loss of epsins impairs UPI peptide effect on tumor angiogenesis.

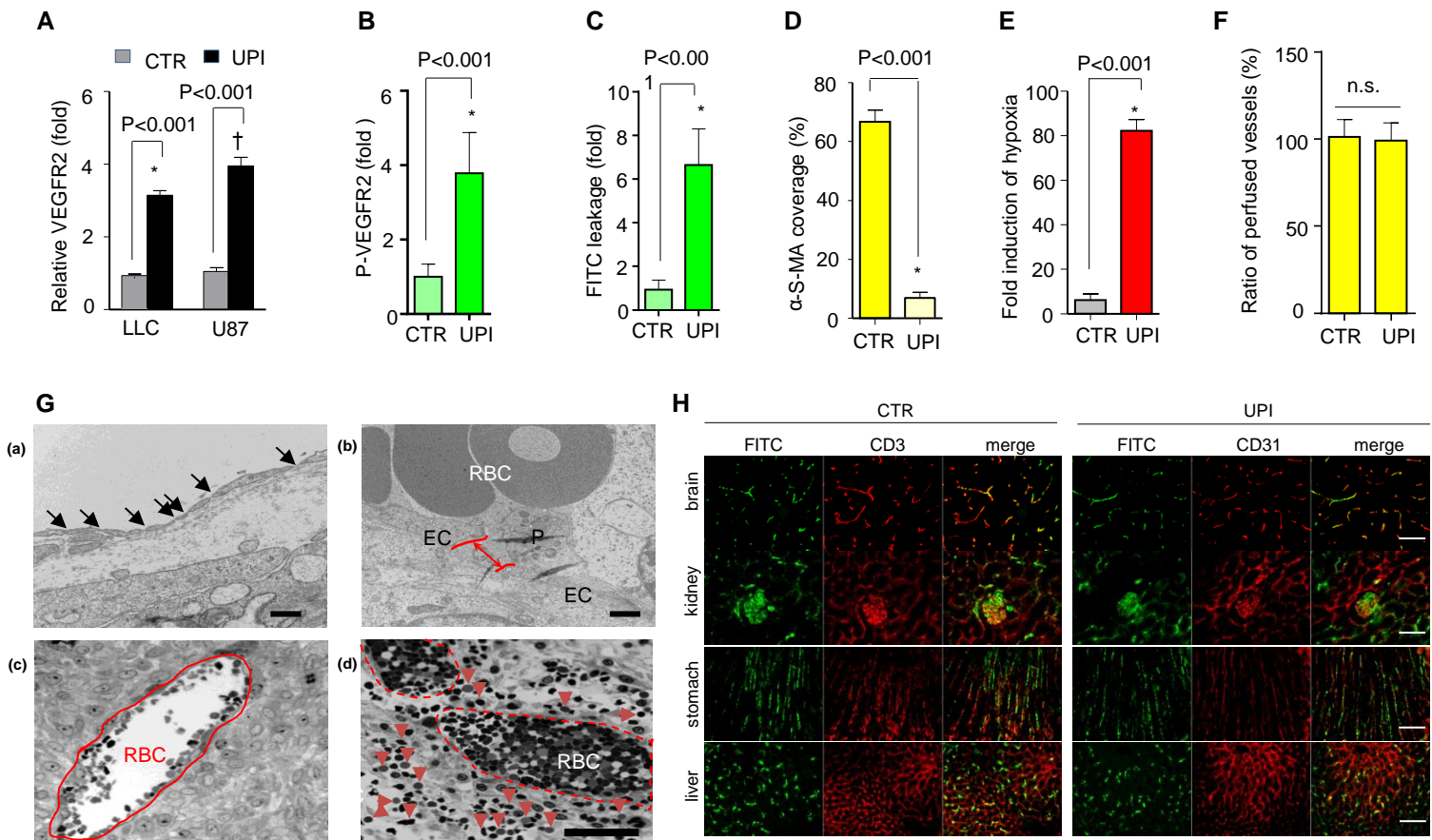


**Supplemental Figure 6. UPI peptide treatment augments tumor angiogenesis revealed by immunostaining using Ve-cadherin antibody in LLC and U87 tumors, related to Figure 7.**

(A). Representative immunofluorescent staining using anti-Ve-Cadherin antibody; n=5; scale bar: 200 µm.

(B). Fold change of vessel density; CTR vs. UPI, \* P<0.001;

(C). Diameter of vessel. n=5. CTR vs. UPI; # P<0.001.



**I** Table: UPI peptide toxicity assay-plasma biomarkers.

	ALB (U/dL)	AST (U/L)	ALT (U/L)	BUN (mg/dL)	CK (U/L)	CREA (mg/dL)	GGT (U/L)	LDH (U/L)	TBIL (mg/dL)
PBS Ctr	2.0 ± 0.2	66.5 ± 2.1	63.5 ± 20.5	20.0 ± 2.0	201.5 ± 33.2	0.170 ± 0.01	<5	525.5 ± 62.9	<0.1
10mg/kg	1.98 ± 0.1	62.3 ± 3.6	63.5 ± 10.8	18.0 ± 0.8	163.5 ± 50.0	0.173 ± 0.02	<5	397.8 ± 26.0	<0.1
25mg/kg	2.0 ± 0.1	55.0 ± 5.3	65.3 ± 4.0	18.7 ± 2.5	165.7 ± 8.6	0.160 ± 0.02	<5	365.7 ± 77.9	<0.1
50mg/kg	2.2 ± 0.2	52.0 ± 4.4	71.7 ± 6.0	21.0 ± 2.0	153.7 ± 33.9	0.180 ± 0.02	<5	481.5 ± 12.1	<0.1
P value*	0.8457	0.154	0.8652	0.1233	0.3985	0.8322	N/A	0.189	N/A

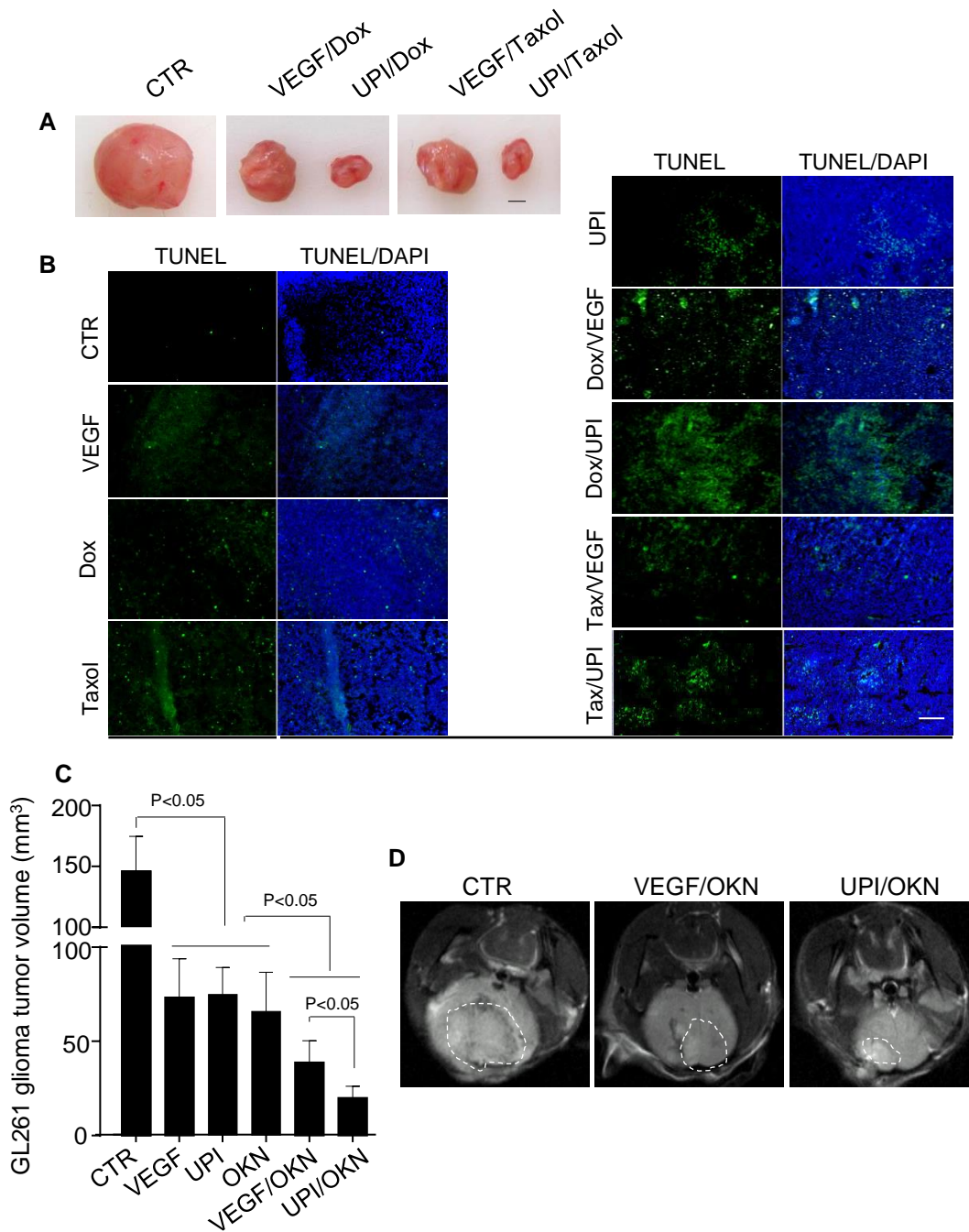
**Supplemental Figure 7. UPI peptide increases tumor vessel permeability and leakage, but does not cause vessel leakage in other major organs (non-tumor organs), related to Figure 7.**

(A-F) Quantifications for Figure 6D (VEGFR2), 6E (P-VEGFR2), 6F (vessel permeability), 6G ( $\alpha$ -SMA coverage), 6I (tumor hypoxia) and 6J (% of perfused vessel in intestine), respectively; n>5.

(G) Tumors collected from UPI peptide treated U87/SCID animal models were prepared for TEM analysis. (a) Representative image of UPI peptide treated U87 tumor depicting fenestration in the endothelium; indicated by black arrows; (b) Representative image of UPI peptide treated U87 tumor showing platelet aggregations in an open junction (red arrow) between two ECs. RBC: red blood cell; P: platelet; EC: endothelial cells; (c) Representative image taken from U87 control tumor, showing red blood cells are inside vessels; (d) Representative image of UPI peptide treated U87 tumor showing increased permeability and significant RBC leakage in semi-thin sections (red arrowheads); n=5 for all data; Scale bar (a, b): 500nm; (c, d): 100 $\mu$ m.

(H) B16-melanoma tumor bearing mice were i.v.-injected with control or UPI peptides for 16 days (dosage: 10mg/kg, every-other-day). Mice were perfused with FITC-Dextran injection for 10min. Tumors and other major organs were harvested and fixed for CD31 staining. FITC (green) and CD31 (red) were visualized simultaneously by confocal microscopy. Data showing no leakage in all examined non-tumor organs; n=3; Scale bar: 100 $\mu$ m.

(I) Mice were i.v.-injected with different dosage of UPI peptides for 3 months and blood serums were subjected to biochemical test by UT Southwestern service facility at Dallas, TX; n=5.



**Supplemental Figure 8. UPI peptide has increased efficacy when combined with cytotoxic chemotherapeutics; related to Figure 9.**

(A) Representative images of tumors from subcutaneous LLC tumor-bearing mice treated with anti-VEGF/Dox, UPI/Dox, anti-VEGF/Taxol or UPI/Taxol, n=6; Scale Bar: 4mm.

(B) Representative TUNEL Staining of LLC tumors shown in (A), n=6; Scale bar: 100µm.

(C-D) Quantification (C) and representative images (D) of orthotopic GL261 tumor-bearing mice treated with UPI/OKN versus anti-VEGF/OKN. Dosages used: intravenous injection of 5 mg/kg UPI or 2.5 mg/kg anti-VEGF antibody every-second-day, and 0.1% OKN-007 (w/v or 75 mg/kg/day) in drinking water., n=5; P<0.05. Data is taken at post-implantation Day-23.

**Supplemental Table 1: Peptides used in this study (Related to all Figures )**

Name of peptide	Tracking marker at the N-terminal	Chimeric UIM peptide	Full UIM peptide sequences**	Total number of amino acids
AP-UIM	±FITC	(F)-AP-UIM	(Fluo-)- <i>RQIKIWFQNRRMKWKK</i> SGEEELQLQLALAMSKEE	34
[F]UI	±FITC	(F)-UIM-iRGD <sup>†</sup>	(Fluo-)- SGEEELQLQLALAMSKEE CRGDKGPDC	27
[F]UPI	±FITC	(F)-UIM-PM-iRGD <sup>†</sup>	(Fluo-)- SGEEELQLQLALAMSKEE MGCISKRKCRGDKGPDC	36
UPI-Δ-Ub (Epsin Ub binding deficient UIM)	N/A	UIM*-PM-iRGD	SGEEELQLQAMSKEEMGCISKRKCRGDKGPDC	33
UPI-mut (Triple mutant)	N/A	UIM**-PM-iRGD	SGEEELQLALALSMSAEE MGCISKRKCRGDKGPDC	36
Hrs-UIM	N/A	Hrs-UIM-PM-iRGD	QEEEEQLALALSQSEAEEMGCISKRKCRGDKGPDC	38
Eps15-UIM	N/A	Eps15-UIM-PM-iRGD	SEEDMIEWAKRESEREEEEQRMGCISKRKCRGDKGPDC	38
Control peptide1	±FITC	(F)-Scrambled-control-1	(Fluo-)- QSLQESGMELEAELALEK** MGCISKRKCRGDKGPDC	36
Control peptide2	±FITC	(F)-Scrambled-control-2	(Fluo-)- <i>RQIKIWFQNRRMKWKK</i> QSLQESGMELEAELALEK***	34

AP: *Italics* and **Black**; Red: UIM; Green: iRGD; Blue: PM anchoring peptide

UIM\*\* indicating triple mutation (Q9→A9, A13→S13, K16→A16)

\*\*\* Scrambled UIM peptide; † iRGD is cyclic.